



# Measuring the subgingival microbiota in periodontitis patients: Comparison of the surface layer and the underlying layers

Guojing Liu<sup>1</sup> | Feng Chen<sup>2</sup> | Yu Cai<sup>1</sup> | Zhibin Chen<sup>1</sup> | Qingxian Luan<sup>1</sup> | Xiaoqian Yu<sup>1</sup>

<sup>1</sup>Department of Periodontology, Peking University School and Hospital of Stomatology, Beijing, China

<sup>2</sup>Central Laboratory, Peking University School and Hospital of Stomatology, Beijing, China

## Correspondence

Xiaoqian Yu, Department of Periodontology, Peking University School and Hospital of Stomatology, 22 Zhong-Guan-Cun South Avenue, Haidian District, Beijing 100081, China.  
Email: y\_pk@163.com

## Funding information

National Natural Science Foundation of China, Grant/Award Number: 81470740

## Abstract

Periodontitis is a major cause of tooth loss in adults that initially results from dental plaque. Subgingival plaque pathogenesis is affected by both community composition and plaque structures, although limited data are available concerning the latter. To bridge this knowledge gap, subgingival plaques were obtained using filter paper (the fourth layer) and curette (the first-third layers) sequentially and the phylogenetic differences between the first-third layers and the fourth layer were characterized by sequencing the V3–V4 regions of 16S rRNA. A total of 11 phyla, 148 genera, and 308 species were obtained by bioinformatic analysis, and no significant differences between the operational taxonomic unit numbers were observed for these groups. In both groups, the most abundant species were *Porphyromonas gingivalis* and *Fusobacterium nucleatum*. *Actinomyces naeslundii*, *Streptococcus intermedius*, and *Prevotella intermedia* possessed relatively high proportions in the first-third layers; while in the fourth layer, both traditional pathogens (*Treponema denticola* and *Campylobacter rectus*) and novel pathobionts (*Eubacterium saphenum*, *Filifactor alocis*, *Treponema sp.* HOT238) were prominent. Network analysis showed that either of them exhibited a scale-free property and was constructed by two negatively correlated components (the pathogen component and the nonpathogen component), while the synergy in the nonpathogen component was lower in the first-third layers than that in the fourth layer. After merging these two parts into a whole plaque group, the negative/positive correlation ratio increased. With potential connections, the first-third layers and the fourth layer showed characteristic key nodes in bacterial networks.

## KEYWORDS

periodontitis, plaque layers, sequencing, subgingival microbiota

**Abbreviations:** ANCOVA, analysis of covariance; ANOSIM, analysis of the similarities; BI, bleeding index; CAL, clinical attachment loss; FISH, fluorescent in situ hybridization; LDA, linear discriminant analysis; LEfSe, linear discriminant analysis effect size; OTU, operational taxonomic unit; PCoA, principal coordinate analysis; PD, probing depth; PII, plaque index.

## 1 | INTRODUCTION

Periodontitis is the sixth most prevalent disease and a major cause of tooth loss in adult populations worldwide.<sup>1,2</sup> As reviewed in previous studies, it is a bacterial plaque-induced inflammatory disease of the periodontal tissue,<sup>3-6</sup> while the pathogenesis of subgingival plaque is affected by the community composition as well as the plaque structure.<sup>7</sup> Over the decades, different technics have been applied by researchers to clarify dental plaque structures, from scanning electron microscopy to immunohistochemical staining, and fluorescent *in situ* hybridization (FISH). Four different layers were distinguished in subgingival plaques: the first to the third layers were located on the tooth surface and embedded in the intercellular matrix, while the fourth layer was a loose layer without clear organization between the attached biofilm and the soft tissue.<sup>7</sup> Up to 15 taxa could be differentiated simultaneously using combinatorial labeling and the spectral imaging-FISH technique, whereas this number is still very limited compared with that of more than 200 taxa that have been detected in subgingival plaques.<sup>8-11</sup> The other barrier in the subgingival plaque structure study is in the mature subgingival plaque accessing, particularly for the surface layer.<sup>12</sup> Until now, tooth extraction is the only method to obtain undisturbed natural subgingival plaques, which is unrepeatable and could only be applied to a hopeless tooth.

Compared with traditional microbial detection technics, sequencing has prompted the recognition of the subgingival community. This open-ended method not only emphasized the importance of assessing the entire microbiota, but also enabled less-biased analysis of the community composition of the plaque structure.<sup>13-15</sup> In this study, the first–third layers and the fourth layer of subgingival plaques were obtained separately using different sampling methods followed by high-throughput sequencing to clarify the characteristics and the connections of these two parts.

## 2 | MATERIALS AND METHODS

### 2.1 | Participant selection

The protocol for this study was approved by the Ethics Committee of Peking University School and the Hospital of Stomatology (PKUSSIRB-201525102). Informed consent was obtained from all the participants according to the Declaration of Helsinki.

Twelve individuals were recruited from the Department of Periodontology at the Peking University Hospital of Stomatology between April 2016 and August 2016.

Individuals were (a) 18–35 years of age, (b) exhibited generalized Stage III to IV, Grade C periodontitis,<sup>16</sup> and

(c) had a minimum of four teeth in both the upper and lower anterior region as well as a minimum of two teeth in each posterior region (upper-right, upper-left, lower-right, and lower-left) with clinical attachment loss (CAL) and a probing depth (PD) of  $\geq 4$  mm.

Patients who were smokers, pregnant or lactating or who had received subgingival periodontal treatment or antibiotic therapy medication within the previous 6 months were excluded from this study.

### 2.2 | Experiment design and sampling

Before this study, oral hygiene instructions and supra-gingival scaling were provided to all of the participants. Participants were examined 1 week after supragingival scaling. The bleeding index (BI),<sup>17</sup> plaque index (PII), probing depth (PD), and clinical attachment loss (CAL) were recorded at six sites for each tooth.

One week after the examination, 16 sites representing four locations (four sites at each location) with  $3 \text{ mm} < \text{PD} < 7 \text{ mm}$  in each patient were selected. These four locations were the buccal-middle sites of posterior teeth (number 3, 4, 19, 20), the buccal-mesial sites of posterior teeth (number 13, 14, 29, 30), the buccal-middle sites of anterior teeth (number 7, 8, 23, 24), and the buccal-mesial sites of anterior teeth (number 9, 10, 25, 26). The subgingival plaques were collected and pooled into four subgingival samples. Had the indicated tooth not qualified, the adjacent tooth would have been selected.

Subgingival plaques were harvested using filter paper strips and curettes sequentially. After saliva isolation, a  $2 \times 10 \text{ mm}$  filter paper (Whatman Grade 3, Whatman International Ltd, Maidstone, UK) was inserted into the pocket bottom for 30 s and transferred into a sterile Eppendorf tube (the fourth layer). The second sample at the same site was obtained with a sterile Gracey curette scratching against the tooth slightly from the bottom of the pocket and was transferred into a sterile Eppendorf tube (the first–third layers). Two hundred microliters of phosphate-buffered saline was added into the sample tubes and the tubes were vibrated for 1 hr. All the samples were centrifuged and stored at  $-80^\circ\text{C}$ .

### 2.3 | DNA extraction and sequencing

DNA was extracted with lysozyme (20 mg/mL) and proteinase K (200  $\mu\text{g}/\text{mL}$ ) using a QIAamp DNA Mini Kit (Qiagen, Hilden, Germany) following the manufacturer's directions. The V3-V4 16S rRNA hypervariable region was amplified with the primers 338F (5'-ACTCCTACGGGAGGCAGCAG-3') and 806R (5'-GGACTACHVGGGT

WTCTAAT-3') linked to barcode sequences. Polymerase chain reaction (PCR) was performed as follows: 94°C for 5 min; followed by 30 cycles of 95°C (30 s), 56°C (30 s), and 72°C (40 s); and a final extension step at 72°C (10 min). A QIAquick Gel Extraction Kit (Qiagen) was used to purify the PCR products, and sequencing was performed on a MiSeq platform (Auwigene Co., Beijing, China).

## 2.4 | Data access

The datasets generated in this study are available in the NCBI Sequence Read Archive under the accession number SRP102224.

## 2.5 | Sequence data processing and analysis

QIIME version 1.9.1<sup>18</sup> and Mothur version 1.35.0<sup>19</sup> were used to analyze the sequence data, and SPSS version 22 (SPSS Inc., Chicago, IL) was used for statistical analyses. Different samples were isolated with specific barcode sequences. After trimming off the primer and barcode sequences, high-quality sequences were clustered into operational taxonomic units (OTUs) using Usearch<sup>20</sup> with 97% similarity. Taxonomy was assigned based on the RDP classifier version 2.12 (*-assignment method*) and Human Oral Microbiome Database 14.5 (*-reference\_seqs\_fp*) with >70% confidence under the script of *assign\_taxonomy* in QIIME.<sup>21</sup> To assign to species level, L7 was imputed under *summary\_taxa.py*. For each OTU, if more than one taxon with >0.7 confidence was assigned in species level, a higher taxonomical level (genus level) would be checked and the highest taxonomical level at which only one taxon could achieve >0.7 confidence would be assigned. The details of the confidence of all taxonomies are attached in Table S1. Shannon index, Simpson index, observed species, Chao1 and a phylogenetic diversity whole tree were chosen to represent alpha diversity and were compared by performing a Mann-Whitney U-test between the two groups. Based on the matrix of the distance and the UniFrac distance, weighted principal coordinate analysis (PCoA) and analysis of the similarities (ANOSIM) was performed.<sup>22</sup> Taxa differentiating the first–third layers and the fourth layer were identified using the linear discriminant analysis (LDA) effect size (LEfSe) method.<sup>23</sup> A Box-Cox normality plot was used to transform the sequencing data, and analysis of covariance (ANCOVA) was performed to detect taxa with differences in the mean abundance between the two groups by adjusting the sampling location. The obtained

*P* values were adjusted using the q-value package in R version 3.3.<sup>24</sup> For correlation analysis, all sequences of the two parts from the same location in each participant were merged as a third group, which was named the whole plaque group. Following a similar cluster and classifying procedure, OTUs with a prevalence higher than 50% in each of the three groups were selected for Spearman correlation analysis. Connections with  $|R| > 0.6$  and  $p < .01$  were used to construct the correlation networks using Cytoscape version 3.3. Corresponding random networks with the same node number were generated using the Erdos-Renyi model on the Network Randomizer 1.1.3 in Cytoscape.<sup>25</sup> Topological features, including the clustering coefficient and the average shortest path length, were calculated using Network Analyzer in Cytoscape.

## 3 | RESULTS

Twelve patients were recruited in this study with a mean age of 30.75 years. The clinical and demographic parameters are shown in Table 1, in which the average probing depth was 4.99 mm. Ninety-six pooled samples were obtained and sequenced, and two samples (one sample in each group) did not yield enough PCR products. The samples produced 3,399,542 sequences with an average of 36,165 sequences per sample. These sequences were clustered into 687 OTUs in which 565 and 622 OTUs were identified from the first–third layers and the fourth layer, respectively. No significant difference in OTU numbers was observed between the two groups ( $P = .813$ , independent Student's *t*-test). The most abundant phyla in the first–third layers were *Bacteroidetes* (23.8% of sequences), *Firmicutes* (23.5% of sequences), *Proteobacteria* (15.6% of sequences), *Fusobacteria* (13.8% of sequences), and *Actinobacteria* (12.2% of sequences). In the fourth layer, the predominant phyla

**TABLE 1** Demographic and clinical data for the 12 participants

Male/Female	5/7
Mean age (years)	30.75 ± 3.17
BI (sampling teeth)	3.25 (2.81, 4.00)
PD (sampling teeth, mm)	4.99 ± 1.41
CAL (sampling teeth, mm)	5.13 ± 1.63
BI (full mouth)	3.79 (2.92, 4.00)
PD (full mouth, mm)	4.95 ± 0.66
PII (full mouth)	1.15 (0.88, 1.28)

Values are the mean ± standard deviation or median value (interquartile range).

Abbreviations: BI, bleeding index; CAL, clinical attachment loss; PD, probing depth; PII, plaque index.

were *Firmicutes* (23.4% of sequences), *Bacteroidetes* (21.9% of sequences), *Fusobacteria* (19.8% of sequences), *Proteobacteria* (15.7% of sequences), and *Spirochaetes* (10.8% of sequences). At the genus level, the most abundant genus in the first–third layers were *Fusobacterium* (10.6% of all genera identified), *Porphyromonas* (9.5% of all genera identified), and *Actinomyces* (9.5% of all genera identified), while the most predominant genus in the fourth layer were *Fusobacterium* (16.0% of all genera identified), *Treponema* (10.8% of all genera identified), and *Porphyromonas* (10.3% of all genera identified). A heatmap of the top 10 genera in each sample was also depicted (Figure 1).

There are considerable variations in the bacterial compositions of the samples. Meanwhile, some samples showed similarity in the bacterial correlation. For example, samples with a high proportion of genus *Veillonella* and *Leptotrichia* are usually low in abundance of the genus *Porphyromonas* and *Treponema*.

### 3.1 | Bacterial diversity

Shannon index, Simpson index, Chao1, and observed species were selected as comparisons for diversity, richness, and evenness between the two groups, and no significant difference was demonstrated (Figure 2). Moreover, samples from the four sampling locations within either group exhibited similar bacterial diversity ( $P > .05$ , Kruskal-Wallis test).

Principal coordinate analysis (PCoA) was used to identify similarities/differences in the bacterial composition between the two groups (Figure 3) and showed some overlap in this study. Provided a quantitative measurement of the variations in beta diversity, ANOSIM demonstrated significant differences between the two groups ( $P = .006$ ), while the four sampling locations within each group exhibited no significant differences ( $P = .077, .591$  for the first–third layers and the fourth layer, respectively). Furthermore, hierarchical cluster

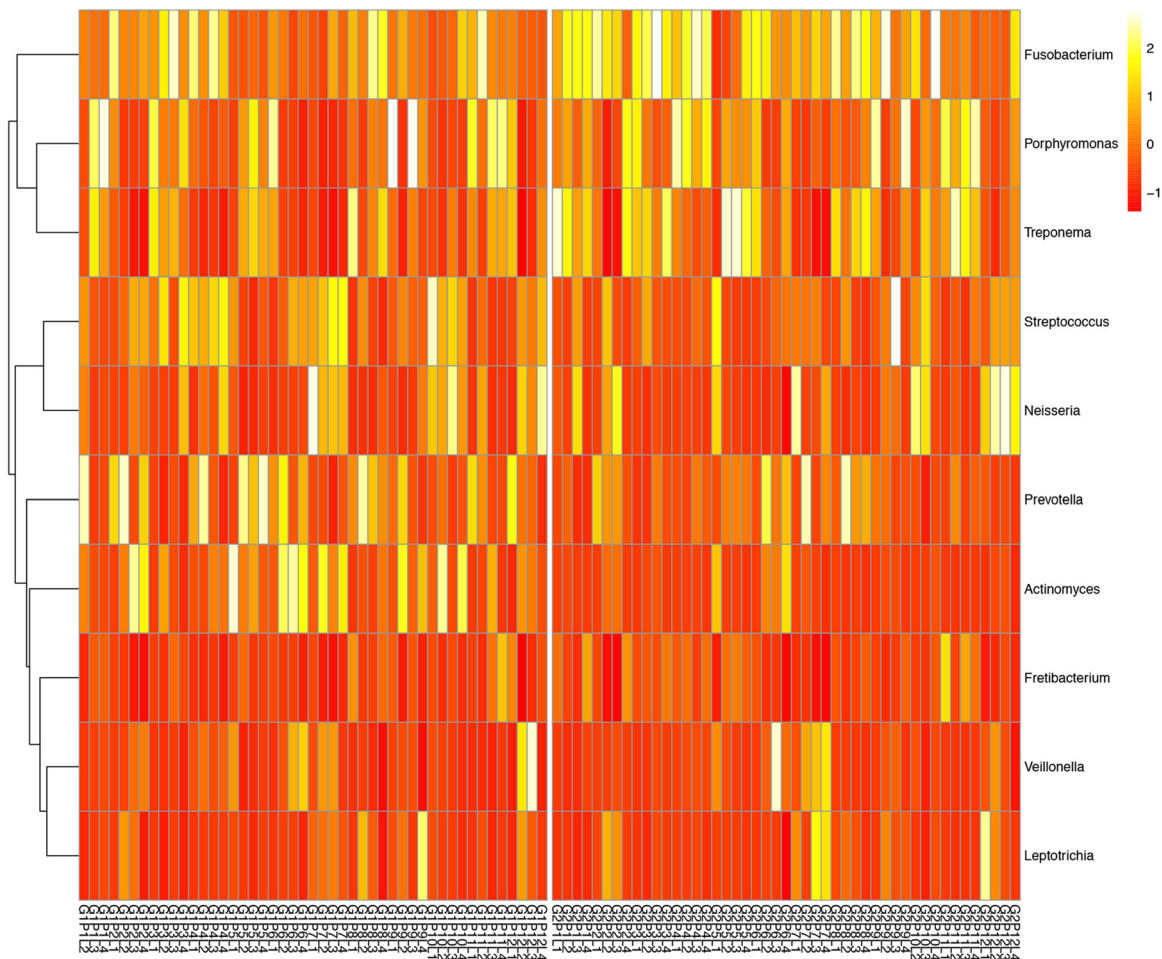


**FIGURE 1** The relative abundances of the top ten genera in the first–third layers and the fourth layer. The relative abundance of each genus is standardized and indicated by the colors. For the labels of the sample: G1, the first–third layers; G2, the fourth layer; P, patient; L1, buccal-middle sites of posterior teeth; L2, buccal-mesial sites of posterior teeth; L3, buccal-middle sites of anterior teeth; L4, buccal-mesial sites of anterior teeth

analysis and a heatmap were conducted and no clear tendency of clustering in samples from the same patient or location was observed (Figures S1, S2).

### 3.2 | Taxonomy analysis

The linear discriminant analysis effect size (LEfSe) determines biomarkers that are most likely to explain the differences between two groups. *Actinobacteria* was the only phylum-level biomarker for the first–third layers, and *Fusobacteria* and *Spirochaetes* were the phylum-level biomarkers for the fourth layer. The genus-level biomarkers in the first–third layers were *Actinomyces* and *Streptococcus*, whereas those in the fourth layer were *Fusobacterium* and *Treponema* (Figure 4).

To further probe differences at species level, ANCOVA was performed adjusting for sampling location. At the genus level, significant differences were observed between *Fusobacterium*, *Treponema*, *Peptostreptococcaceae* [XI][G-5], *Actinomyces*, and *Streptococcus* for the two groups. At species level, *Actinomyces naeslundii*, *Neisseria elongata*, and *Actinomyces sp.* HOT180, were more abundant in the first–third layers, whereas other species, such as *Fusobacterium sp.* HOT203, *Treponema denticola*,

and *Filifactor alocis* were more abundant in the fourth layer (Figure 5).

The relative abundances and prevalences of *Aggregatibacter actinomycetemcomitans* were low and with no significant differences between the groups (0.04% and 0.14% for relative abundance,  $P = .172$ ; 29.78% and 27.66% for prevalence,  $P = .820$ ).

### 3.3 | The core microbiome

Although high inter-sample variation existed in both groups, operational taxonomic units (OTUs) with high abundance and prevalence could still be uncovered to represent the core microbiome in the subgingival community. The OTUs present in most samples (>70% prevalence) were selected, and thresholds of 2%, 1%, and 0.5% were set for further analyses (Figure 6).

With high abundance (>2%), 9 and 12 OTUs were detected as the dominant core members in the first–third layers and the fourth layer, respectively. *Porphyromonas gingivalis*, *Neisseria sicca*, *Fusobacterium sp.* HOT203, *Fusobacterium nucleatum ss. vincentii*, genus *Veillonella*, and *Streptococcus* were selected in both groups. *Prevotella intermedia*, *A. naeslundii*, and *Streptococcus intermedius*

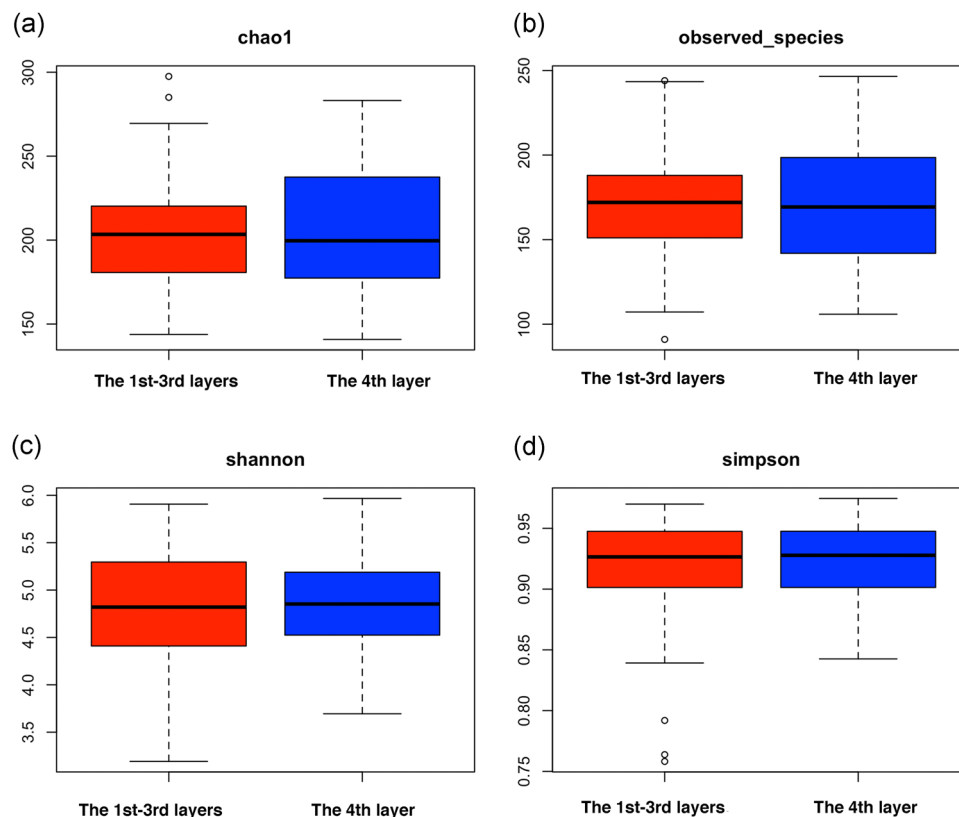


**FIGURE 2** Bacterial diversity of the first–third layers and the fourth layer. Box plots show the Chao1 (a), Observed species (b), Simpson (c), and Shannon indexes (d) between the two groups, with no statistically significant difference between the two groups (Mann-Whitney U-test)



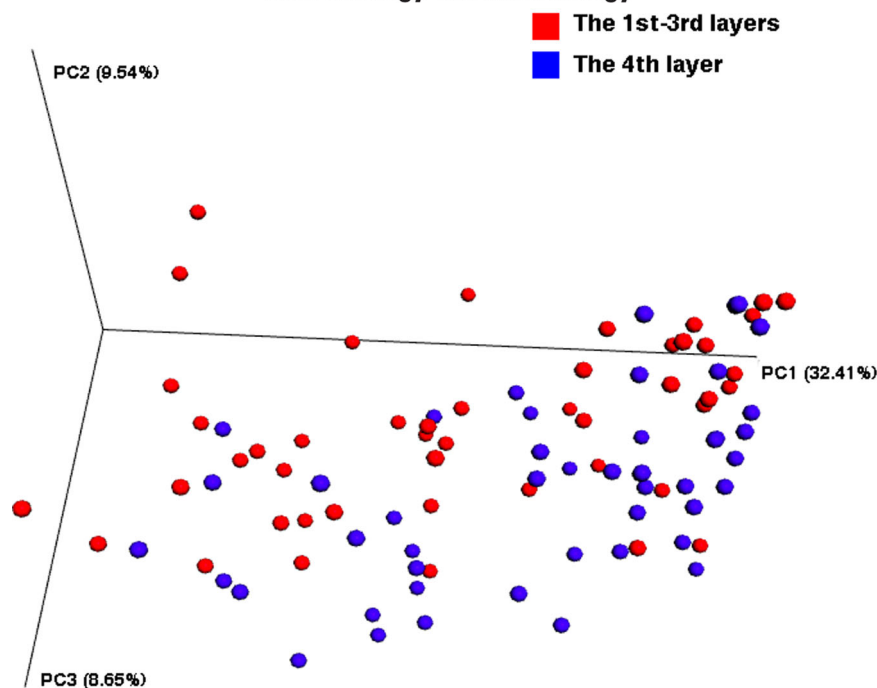


**FIGURE 3** Principal coordinate analysis (PCoA) of the first–third layers and the fourth layer subgingival samples. Each dot represents one sample. Red is the first–third layer samples, blue is the fourth layer samples

were only present in the core microbiome of the first–third layers, while *F. alocis*, *T. denticola*, *Campylobacter rectus*, *Fretibacterium sp.* HOT361, *Eubacterium saphenum*, and *Treponema sp.* HOT238 were only found in the core microbiome of the fourth layer. When the threshold was lowered to 1%, 14 OTUs and 7 OTUs (including *Tannerella forsythia*) were identified as new core members of the first–third layers and the fourth layer. After lowering the threshold to 0.5%, 17 and 20 new core members were included in the first–third layers and the fourth layer, respectively. At this level, the species in the core microbiome for the two groups showed a high degree of similarity (31/39 and 31/38 for the shared/total core members in the first–third layers and the fourth layer).

### 3.4 | Correlation networks

The sequences from the first–third layers and the fourth layer collected at the same sampling sites were merged into new datasets representing the whole plaques. The OTUs with a prevalence higher than 50% in each of these groups (the first–third layers group, the fourth layer group, and the whole plaque group) were selected for correlation analysis, from which we depicted correlation networks (Figure 7). The topological features, including the clustering coefficient and the shortest average path length, were calculated and compared with the corresponding randomized networks with the same node numbers. All these modularity parameters were significantly higher than those from the corresponding randomized networks (Table 2).

The edges/node numbers from the first–third layers, the fourth layer, and whole plaque networks were 783/149, 683/132, and 900/167, respectively, and the distributions of edges were uneven. Being regarded as hubs, the top ten connectivity nodes were directly involved in 29–40% of the correlations in each group, albeit at low proportions (5–8% of all nodes). When we focused on the edges of all the nodes, the numbers of positive correlations (719, 629, 746 edges for the first–third layers, the fourth layer, and whole plaque group) were higher than the numbers of negative correlations (64, 55, 154 edges for the first–third layers, the fourth layer, and the whole plaque group). There are two components existing in each group connected mainly by negative edges. The component consisting mostly of traditional pathogens (*P. gingivalis*, *T. forsythia*, and *T. denticola* etc.) and periodontal pathobionts (phyla *Spirochaetes*, *Synergistetes*, and genus *Peptostreptococcus* etc.) was named the pathogen component, the other component being composed of nonpathogen-related bacteria was named the nonpathogen component in the present study. The nonpathogen component contained more nodes than the other (nonpathogen/total nodes: 93/149, 87/132, 96/167 for the first–third layers, the fourth layer, and the whole plaque).

These data indicated that there were differences in network connections and topological features of the first–third layers and the fourth layer. Focused on the number of neighbors in these networks, both components in the fourth layer network showed similar node connectivity (avg. number of neighbors: 5.3 and 4.5 in pathogen and nonpathogen components). Whereas the

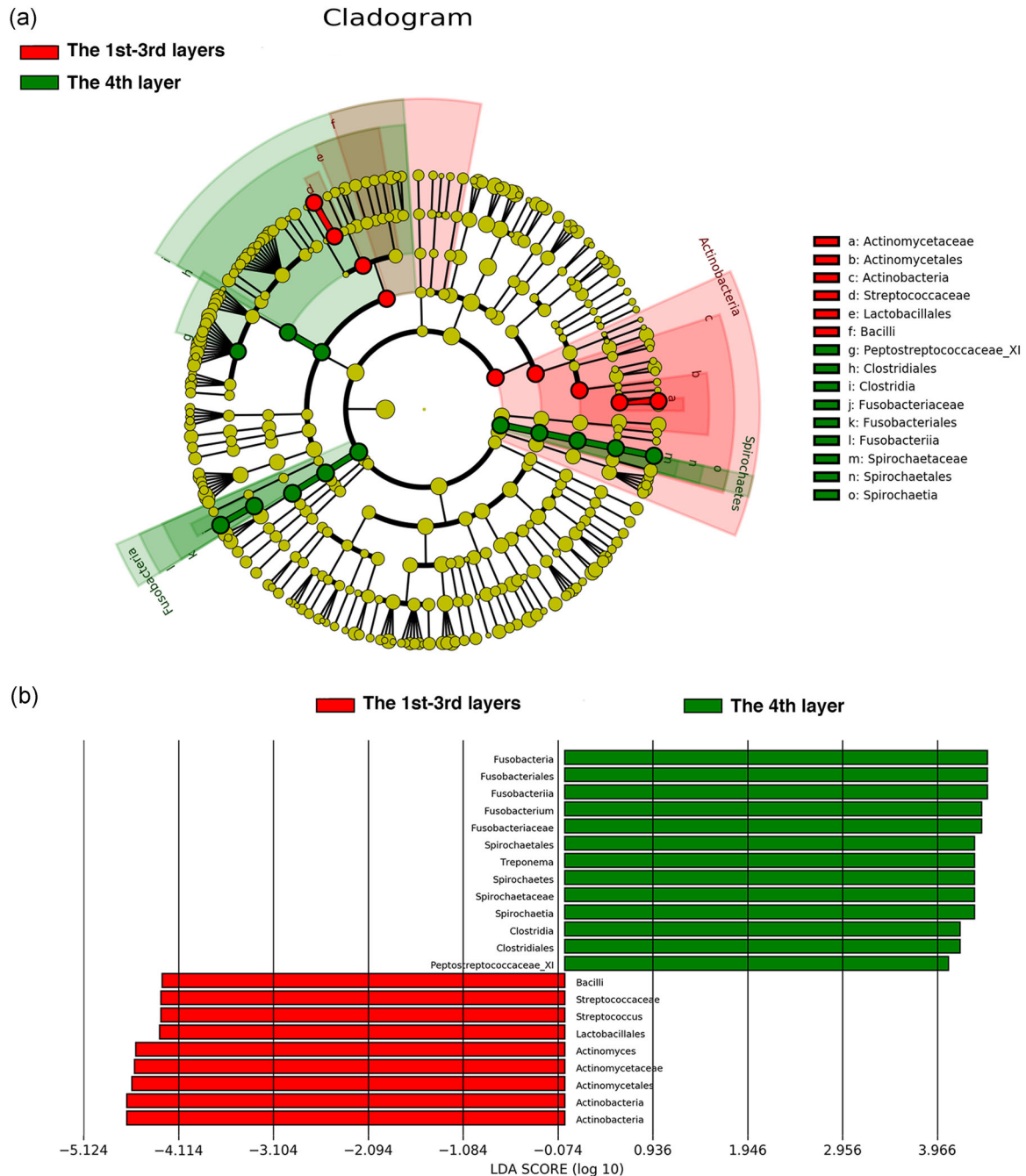


**FIGURE 4** (a) A cladogram of the phylogenetic distribution for the first–third layers (red) and the fourth layer community (green) using linear discriminant analysis effect size (LEfSe). (b) Histogram of the linear discriminant analysis (LDA) scores based on the different abundance between the groups. Bacterial taxa are ranked according to their LDA scores

nodes in the pathogen components presented higher connectivity than those in the nonpathogen component in the first–third layers network (8.1 vs. 2.8). Moreover, hubs were present in both components in the fourth layer network (four hubs in the nonpathogen part and six hubs in the pathogen component) but only existed in the pathogen component in the first–third layer network. After the sequences of the whole plaques were generated, the network exhibited similar

characteristics in terms of node connectivity and hub distribution of the first–third layer network. The topological features were similar among these three networks except for the P/N ratio (positive vs. negative interactions). Compared with the networks of the first–third layers and the fourth layer, the P/N ratios of the whole plaque networks showed a dramatic decrease (11.2, 11.4, and 4.8 for the first–third layer, the fourth layer, and the whole plaque networks).

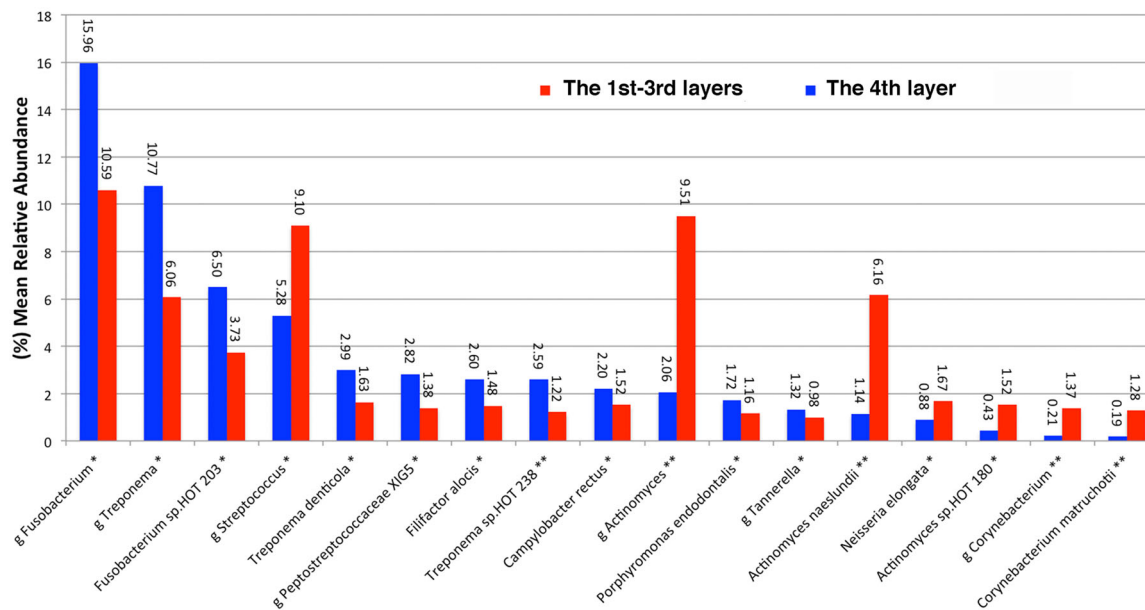


**FIGURE 5** Mean relative abundance of genera and species in the first–third layers and the fourth layer groups (mean relative abundance >1%, significant difference between the two groups: \* $P < .05$ , \*\* $P < .01$ , analysis of covariance)

## 4 | DISCUSSION

Information concerning the community composition and structure are critical to understanding the ecology and physiology characteristics of the subgingival community.<sup>7,26</sup> Sequencing has revolutionized the study of subgingival community compositions, but the positional information of the subgingival bacteria is still very limited due to staining and sampling methods.<sup>15,27</sup> Immunohistochemical staining techniques, FISH, and Combinatorial Labelling and Spectral Imaging-FISH could identify positional information of the bacteria but the taxa numbers revealed simultaneously are constrained by technical limitations (up to 15 taxa).<sup>7,26,28,29</sup> In this study, we collected subgingival plaques sequentially using filter paper and curettes and analysed them separately by sequencing. Although it is a relatively rough method for partitioning the first–third layers and the fourth layer, this combination provides us with additional information about the subgingival community. Using high throughput sequencing, our results showed that the first–third layers and the fourth layer presented notable differences in community compositions and bacterial correlation patterns, connections between these two parts, as well as similarities in bacterial diversity.

### 4.1 | Structure and diversity of bacterial communities

Sequencing has revealed a broad range of taxa in the oral cavity. As reviewed by Human Oral Microbiome Database,

688 taxa have been detected in the oral cavity.<sup>21</sup> This study detected a total of 11 phyla, 26 classes, 44 orders, 79 families, 148 genera, and 308 species-level taxa, which is comparable to previous sequencing studies.<sup>15,30</sup>

Diversity analyze reveals the species number and the composition of a community. The similarities in diversity indicated similarities of bacterial biomass and composition between the first–third layers and the fourth layer. Communities with higher diversity are more robust to change and are associated with a more stable and healthy status.<sup>31,32</sup> The similarities in diversity suggest that the fourth layer might possess a stability that is comparable to that of the first–third layers. As stability could also be affected by other factors, such as functional gene diversity and response diversity, further investigations are needed to complete an integrated picture.<sup>33,34</sup>

### 4.2 | Taxonomy analysis

The spatial organization of the subgingival plaque microbiota is critical to understanding the ecology, physiology, and functional characteristics of the community. The ten most abundant OTUs in each group were identified, among which six OTUs were identical. *P. gingivalis* and *F. nucleatum*, both with significant virulence properties, were the most dominant OTUs in both groups. Kolenbrander found that *F. nucleatum* coaggregates with both early and late colonizers and are essential to oral biofilm establishment.<sup>35–37</sup> *P. gingivalis* alters the subgingival composition to favor



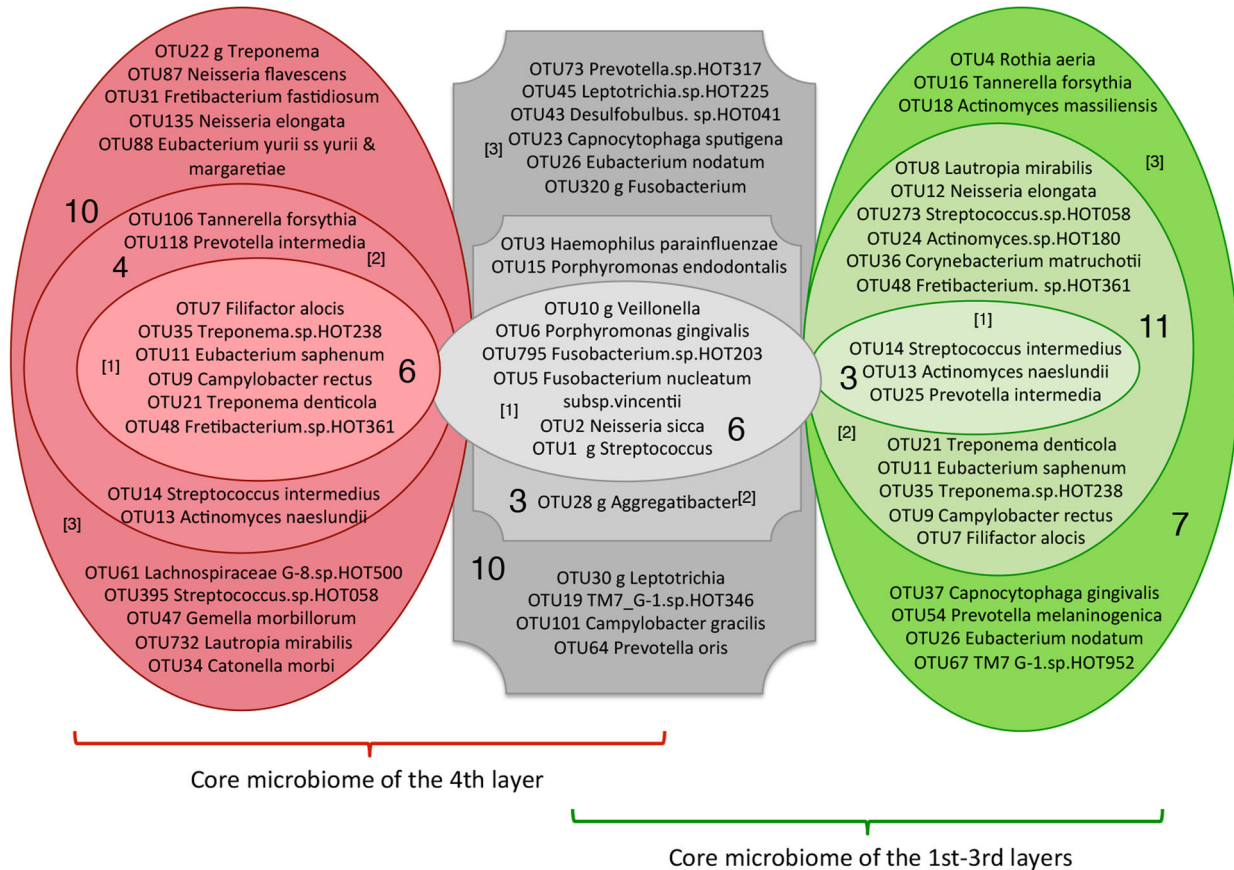


**FIGURE 6** Venn diagram of the core subgingival microbiome in the two groups. Each circle contains operational taxonomic units (OTUs) present in at least 70% of samples within a group. The grey region includes the core subgingival OTUs present with equal prevalence and the relative abundance between the two groups. OTUs in green represent the first–third layers-associated core species, with higher abundance in the first–third layers; OTUs in red represent the fourth layer-associated core species, which show an increased relative abundance in the fourth layer. Inner circles labeled 1 contain highly prevalent and highly abundant OTUs (present in at least 70% of samples from each group and numerically dominant with a mean relative abundance of  $\geq 2\%$  of total sequences). Middle circles labeled 2 contain OTUs that are highly prevalent but present in low abundance (present in 1–2% of total sequences). Outer circles labeled 3 contain OTUs present in low abundance (present in 0.5–1% of total sequences)

more anaerobic microbiota and to impair the host defense by reducing neutrophil infiltration, which leads to bone resorption. Based on this pathogenicity, previous studies have proposed *P. gingivalis* as a keystone pathogen in periodontitis.<sup>5,38</sup> These results agree with previous sequencing studies in which the abundance of periodontal pathogens were similar using either curette or paper-based sampling methods.<sup>13,15,30,39</sup> Similarly, other taxa, such as *Fusobacterium sp.* HOT203, *N. sicca*, genus *Streptococcus*, and the genus *Veillonella*, also exhibit high abundance in both groups. These species might be related to spatial structure organization and biofilm formation.<sup>26,40–42</sup>

There were also some discrepancies between these two groups. The genera *Actinomyces*, *Streptococcus*, and *Corynebacterium*, especially *A. naeslundii* and *S. intermedius*, were strongly associated with the first–third layers, as their relative abundance was

higher in the first–third layers than in the fourth layer. *A. naeslundii* and the genus *Streptococcus* are early colonizers and might play a role in plaque attachment.<sup>41,43</sup> As *Corynebacterium* is the foundational bacterium of the consortium, the higher abundance of these taxa implied a more structured community than the fourth layer.<sup>26</sup> On the contrary, *Fusobacterium* and *Spirochetes* are phylum-level biomarkers for the fourth layer and are present at higher relative abundances. For example, the relative abundance of *T. denticola* was doubled in the fourth layer. It could evade host immune responses via various mechanisms, such as TLR activation, inhabitation, neutrophil polarization, and chemotaxis inhabitation.<sup>44–46</sup> It also exhibits motility and chemotaxis. All these characteristics facilitated this bacterium to penetrate deep pockets and colonize new sites.<sup>47</sup> Using molecular sequencing, we also found that the abundance of

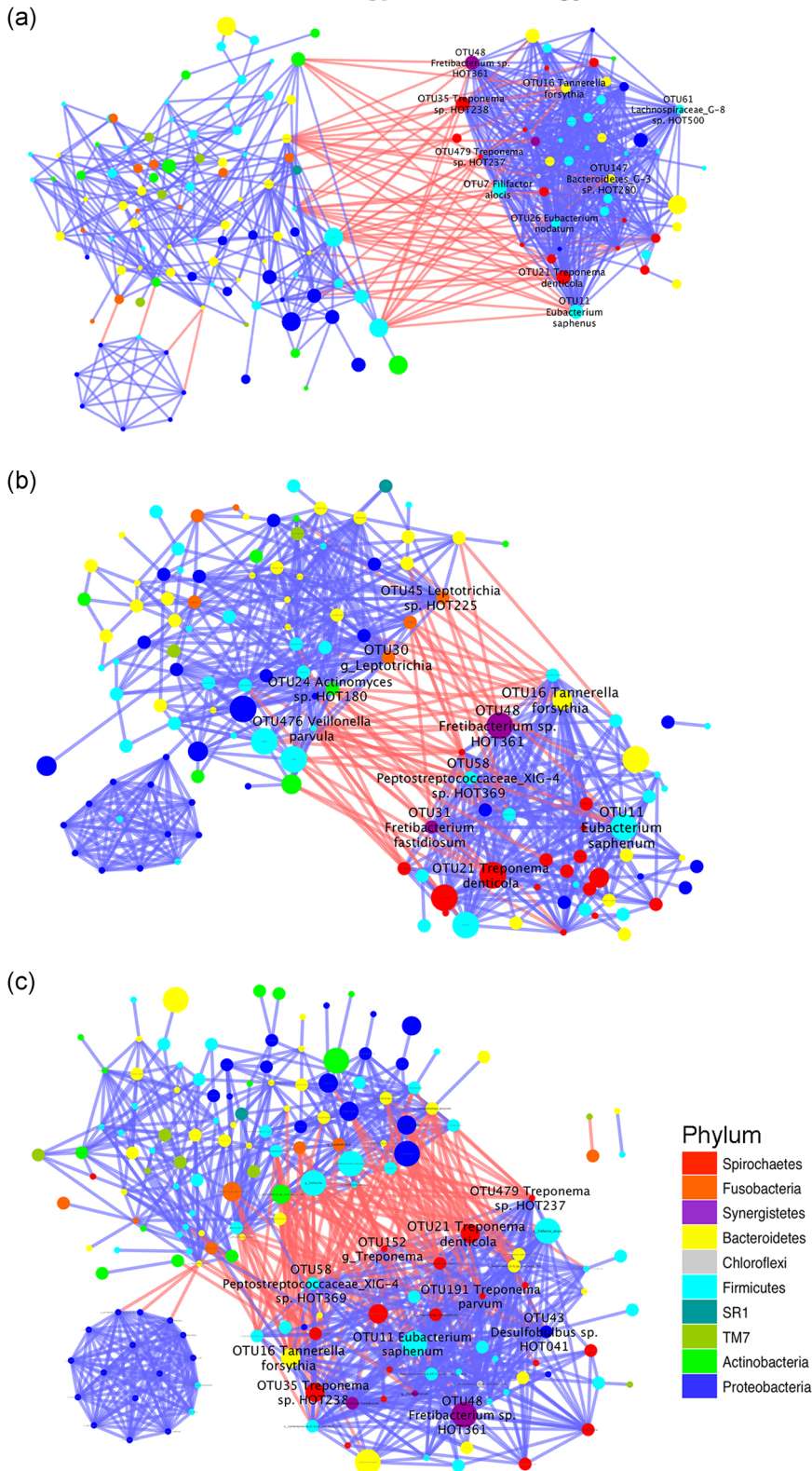


**FIGURE 7** Correlation networks for the first–third layers (a), the fourth layer (b), and whole (c) plaque groups. Each node denotes a microbial taxon. The size of the node depends on relative abundance, and node color indicates the phylum of the taxa. Each edge denotes significant correlations ( $|R| > 0.6$ ,  $P < .01$ , Spearman correlation analysis). Blue indicates positive correlations, and red indicates negative correlations. Nodes with top ten connectivity are labeled by the taxon name

*Synergistes*, *F. alocis*, and *E. saphenum* increased significantly in the fourth layer. As these bacteria were highly prevalent and abundant in periodontitis in previous sequencing studies, they were also suggested to be regarded as periodontal pathogens with moderate evidence.<sup>10,13,14</sup>

All the participants in this study were suffering from aggressive periodontitis according to the 1999 classification.<sup>48</sup> The prevalence and relative abundance of *A. actinomycetemcomitans* in our study are relatively low when compared with other studies (0.14% and 0.04% for relative abundance, 27.66% and 29.78% for

**TABLE 2** Comparison of topological features between real networks and randomized networks with the same node numbers

	The first–third layers		The fourth layer		Whole plaque group	
	Real network	Randomized network	Real network	Randomized network	Real network	Randomized network
Num. of nodes	149	149	132	132	167	167
Num. of edges	783	560.0 ± 18.8	684	435.8 ± 29.8	900	687.4 ± 34.9
Clustering coefficient	0.484	0.053 ± 0.001	0.505	0.042 ± 0.009	0.475	0.049 ± 0.004
Ave. shortest path length	3.80	2.684 ± 0.033	3.32	2.783 ± 0.089	3.49	2.656 ± 0.054
P/N ratio	11.2	–	11.4	–	4.8	–
<b>Pathogen part</b>						
Num. of nodes	56		45		71	
Num. of edges	459		240		435	
E/N ratio	8.1		5.3		6.1	
Sum. relative abundance (%)	26.6		33.7		29.9	
<b>Non-pathogen part</b>						
Num. of nodes	93		87		96	
Num. of edges	260		389		307	
E/N ratio	2.8		4.5		3.2	
Sum. relative abundance	52.8		33.1		33.2	

Values in the randomized networks are the means ± standard deviation. P/N ratio, positive/negative correlations; E/N ratio, edges/node.

prevalence).<sup>49–51</sup> However, our results are consistent with those studies carried out in Asian populations.<sup>27,52–54</sup> This discrepancy might due to different ethnicities as concluded by most researchers.

### 4.3 | Correlation network analysis

The subgingival community contains various species that are connected by multiple types of interactions, such as mutualism, commensalism, parasitism, predation, amensalism, and competition.<sup>55</sup> Correlation analysis provides a method to identify bacterial interactions in complex microbial communities. Therefore, three correlation networks for the first–third layers, the fourth layer, and the whole plaque groups were obtained and analyzed.

All these networks included two negatively correlated components, namely the pathogen component and the nonpathogen component, while positive correlations are prevail in each single component. In the fourth layer, the positive edge/node ratios are similar and the total abundances are comparable in the pathogen and the nonpathogen components, suggesting a similar synergistic bacteria–bacteria effect for both components. On the contrary, in the first–third layers, the positive edge/node ratio of the pathogen component is three times higher

than that in the nonpathogen component, indicating an enhanced synergistic effect in the pathogen component. Considering that the total abundance in the pathogen component is only half of that in the nonpathogen component, other mechanisms, such as micron-scale biogeography and environmental drivers, may also play a role in regulating the proliferation of pathogens in subgingival plaques.

The sequence data from the first–third layers and the fourth layer were merged and the OTUs with a prevalence higher than 50% were selected to construct a whole plaque correlation network. An increase of negative correlations in this group were observed compared with the values before merging which suggests a negative correlation between these two parts. As reviewed by Faust in 2012, negative correlations usually result from competition, the prey–predator relationship, and amensalism.<sup>55</sup> However, compositional bias from data merging and sequential sampling should also be considered.

Topological analyses provide an overview of network properties. The coefficient index and average shortest path length of all of the networks (the first–third layers, the fourth layer, and the whole plaque) were calculated, and the topological features of these networks were compared with random networks of the same size. The clustering coefficients and the characteristic path lengths of all the three networks were higher than that in random



networks, and they were within the range of other biological networks displaying scale-free behavior.<sup>56-58</sup> These results indicate that bacteria in these three subgingival networks communicate with other bacteria. The scale-free networks are more robust to changes but more sensitive to removing or changing highly connected nodes (hubs).<sup>59</sup>

The distributions of hubs among those networks are different. The first–third layers-associated hubs only exist in the pathogen component and are positively correlated, which is consistent with the whole plaque group. On the contrary, hubs are present in both components and are connected by positive/negative associations in the fourth layer network. The hubs in the nonpathogen component, such as *Actinomyces sp.* HOT180, *Leptotrichia sp.* HOT225, and *Veillonella parvula*, might possess the ability to inhibit pathogens and to balance subgingival communities.

As shown in the hierarchical cluster analysis and a heatmap, no clear tendency of clustering in samples from the same patient or location was observed. Based on these results and limited number of patients (12 patients), location-based analysis was conducted, which depicted the relations and similarities between these two parts and increased our knowledge of the subgingival plaque. Further research with a larger sampling size should be undertaken to gain much more general conclusions and to elucidate potential individual and location effects in the future.

In conclusion, this study depicted distinct bacteria compositions in the first–third layers and the fourth layer of subgingival plaques. Traditional pathogens (*T. denticola* and *C. rectus*) and novel pathobionts (*E. saphenum*, *F. alocis*, *Treponema sp.* HOT238) are more abundant in the fourth layer, while some genera such as *A. naeslundii*, *S. intermedius*, and *P. intermedia* usually appear in the first–third layers. Either of these two parts exhibits a scale-free property and is constructed by two negatively correlated components (the pathogen component and the nonpathogen component), while the synergy in the nonpathogen component is lower in the first–third layers than that in the fourth layer.

## ACKNOWLEDGMENT

This work was supported by grants from the National Natural Science Foundation of China (81470740).

## CONFLICT OF INTEREST

The authors declare that there are no conflicts of interest.

## ORCID

Guojing Liu  <http://orcid.org/0000-0001-9588-4678>

## REFERENCES

- Marcenes W, Kassebaum NJ, Bernabe E, et al. Global burden of oral conditions in 1990–2010: a systematic analysis. *J Dent Res.* 2013;92:592–7.
- Kassebaum NJ, Bernabe E, Dahiya M, Bhandari B, Murray CJ, Marcenes W. Global burden of severe periodontitis in 1990–2010: a systematic review and meta-regression. *J Dent Res.* 2014;93:1045–53.
- Socransky SS, Haffajee AD, Cugini MA, Smith C, Kent RL Jr. Microbial complexes in subgingival plaque. *J Clin Periodontol.* 1998;25:134–44.
- Darveau RP. Periodontitis: a polymicrobial disruption of host homeostasis. *Nat Rev Microbiol.* 2010;8:481–90.
- Hajishengallis G, Liang S, Payne MA, et al. Low-abundance biofilm species orchestrates inflammatory periodontal disease through the commensal microbiota and complement. *Cell Host Microbe.* 2011;10:497–506.
- Costalonga M, Herzberg MC. The oral microbiome and the immunobiology of periodontal disease and caries. *Immunol Lett.* 2014;162:22–38.
- Zijng V, van Leeuwen MB, Degener JE, et al. Oral biofilm architecture on natural teeth. *PLoS One.* 2010;5:e9321.
- Paster BJ, Boches SK, Galvin JL, et al. Bacterial diversity in human subgingival plaque. *J Bacteriol.* 2001;183:3770–83.
- Sanz-Martin I, Doolittle-Hall J, Teles RP, et al. Exploring the microbiome of healthy and diseased peri-implant sites using Illumina sequencing. *J Clin Periodontol.* 2017;44:1274–84.
- Perez-Chaparro PJ, Goncalves C, Figueiredo LC, et al. Newly identified pathogens associated with periodontitis: a systematic review. *J Dent Res.* 2014;93:846–58.
- Perez-Chaparro PJ, McCulloch JA, Mamizuka EM, et al. Do different probing depths exhibit striking differences in microbial profiles? *J Clin Periodontol.* 2018;45:26–37.
- Zijng V, Ammann T, Thurnheer T, Gmur R. Subgingival biofilm structure. *Front Oral Biol.* 2012;15:1–16.
- Abusleme L, Dupuy AK, Dutzan N, et al. The subgingival microbiome in health and periodontitis and its relationship with community biomass and inflammation. *ISME J.* 2013;7:1016–25.
- Griffen AL, Beall CJ, Campbell JH, et al. Distinct and complex bacterial profiles in human periodontitis and health revealed by 16S pyrosequencing. *ISME J.* 2012;6:1176–85.
- Camelo-Castillo AJ, Mira A, Pico A, et al. Subgingival microbiota in health compared to periodontitis and the influence of smoking. *Front Microbiol.* 2015;6:119.
- Tonetti MS, Greenwell H, Kornman KS. Staging and grading of periodontitis: framework and proposal of a new classification and case definition. *J Periodontol.* 2018;89(Suppl 1):S159–S72.
- Mazza JE, Newman MG, Sims TN. Clinical and antimicrobial effect of stannous fluoride on periodontitis. *J Clin Periodontol.* 1981;8:203–12.
- Caporaso JG, Lauber CL, Walters WA, et al. Ultra-high-throughput microbial community analysis on the Illumina HiSeq and MiSeq platforms. *ISME J.* 2012;6:1621–4.

19. Schloss PD, Westcott SL, Ryabin T, et al. Introducing mothur: open-source, platform-independent, community-supported software for describing and comparing microbial communities. *Appl Environ Microbiol.* 2009;75:7537-41.
20. Edgar RC. Search and clustering orders of magnitude faster than BLAST. *Bioinformatics.* 2010;26:2460-1.
21. Dewhirst FE, Chen T, Izard J, et al. The human oral microbiome. *J Bacteriol.* 2010;192:5002-17.
22. Clarke KR. Nonparametric multivariate analyses of changes in community structure. *Aust J Ecol.* 1993;18:117-43.
23. Segata N, Izard J, Waldron L, et al. Metagenomic biomarker discovery and explanation. *Genome Biol.* 2011;12:R60.
24. Dabney A, Storey JD, Warnes GR (2010). Q-value: Q-value estimation for false discovery rate control. R-package version 1.24.0.
25. Erdős P, Rényi A. On random graphs. *Publ Math-Debrecen.* 1959;6:290-7.
26. Welch JLM, Rossetti BJ, Rieken CW, Dewhirst FE, Borisy GG. Biogeography of a human oral microbiome at the micron scale. *PNAS.* 2016;113:E791-800.
27. Li Y, Feng XH, Xu L, et al. Oral microbiome in Chinese patients with aggressive periodontitis and their family members. *J Clin Periodontol.* 2015;42:1015-23.
28. Listgarten MA, Mayo H, Amsterdam M. Ultrastructure of the attachment device between coccal and filamentous microorganisms in "corn cob" formations of dental plaque. *Arch Oral Biol.* 1973;18:651-6.
29. Noiri Y, Li L, Ebisu S. The localization of periodontal-disease-associated bacteria in human periodontal pockets. *J Dent Res.* 2001;80:1930-4.
30. Bizzarro S, Loos BG, Laine ML, Crielaard W, Zaura E. Subgingival microbiome in smokers and non-smokers in periodontitis: an exploratory study using traditional targeted techniques and a next-generation sequencing. *J Clin Periodontol.* 2013;40:483-92.
31. Lozupone CA, Stombaugh JI, Gordon JI, Jansson JK, Knight R. Diversity, stability and resilience of the human gut microbiota. *Nature.* 2012;489:220-30.
32. Lozupone CA, Hamady M, Kelley ST, Knight R. Quantitative and qualitative beta diversity measures lead to different insights into factors that structure microbial communities. *Appl Environ Microb.* 2007;73:1576-85.
33. Li Y, He J, He Z, et al. Phylogenetic and functional gene structure shifts of the oral microbiomes in periodontitis patients. *ISME J.* 2014;8:1879-91.
34. Mori AS, Furukawa T, Sasaki T. Response diversity determines the resilience of ecosystems to environmental change. *Biol Rev Camb Philos Soc.* 2013;88:349-64.
35. Kolenbrander PE, Palmer RJ Jr., Periasamy S, Jakubovics NS. Oral multispecies biofilm development and the key role of cell-cell distance. *Nat Rev Microbiol.* 2010;8:471-80.
36. Kolenbrander PE, Palmer RJ Jr., Rickard AH, Jakubovics NS, Chalmers NI, Diaz PI. Bacterial interactions and successions during plaque development. *Periodontol 2000.* 2006;42:47-79.
37. Kolenbrander PE, Andersen RN, Moore LV. Coaggregation of *Fusobacterium nucleatum*, *Selenomonas flueggei*, *Selenomonas infelix*, *Selenomonas noxia*, and *Selenomonas sputigena* with strains from 11 genera of oral bacteria. *Infect Immun.* 1989;57:3194-203.
38. Hajishengallis G, Lamont RJ. Beyond the red complex and into more complexity: the polymicrobial synergy and dysbiosis (PSD) model of periodontal disease etiology. *Mol Oral Microbiol.* 2012;27:409-19.
39. Park OJ, Yi H, Jeon JH, et al. Pyrosequencing analysis of subgingival microbiota in distinct periodontal conditions. *J Dent Res.* 2015;94:921-7.
40. Valm AM, Welch JLM, Rieken CW, et al. Systems-level analysis of microbial community organization through combinatorial labeling and spectral imaging. *PNAS.* 2011;108:4152-7.
41. Uzel NG, Teles FR, Teles RP, et al. Microbial shifts during dental biofilm re-development in the absence of oral hygiene in periodontal health and disease. *J Clin Periodontol.* 2011;38:612-20.
42. Palmer RJ, Shah N, Valm A, et al. Interbacterial adhesion networks within early oral biofilms of single human hosts. *Appl Environ Microb.* 2017;83:e00407-17.
43. Li J, Helmerhorst EJ, Leone CW, et al. Identification of early microbial colonizers in human dental biofilm. *J Appl Microb.* 2004;97:1311-8.
44. Brissette CA, Pham TT, Coats SR, Darveau RP, Lukehart SA. *Treponema denticola* does not induce production of common innate immune mediators from primary gingival epithelial cells. *Oral Microbiol Immunol.* 2008;23:474-81.
45. Brissette CA, Lukehart SA. Mechanisms of decreased susceptibility to beta-defensins by *Treponema denticola*. *Infect Immun.* 2007;75:2307-15.
46. Nussbaum G, Ben-Adi S, Genzler T, Sela M, Rosen G. Involvement of Toll-like receptors 2 and 4 in the innate immune response to *Treponema denticola* and its outer sheath components. *Infect Immun.* 2009;77:3939-47.
47. Charon NW, Goldstein SF. Genetics of motility and chemotaxis of a fascinating group of bacteria: the spirochetes. *Annu Rev Genet.* 2002;36:47-73.
48. Armitage GC. Development of a classification system for periodontal diseases and conditions. *Ann Periodontol.* 1999;4:1-6.
49. Bonta Y, Zambon JJ, Genco RJ, Neiders ME. Rapid identification of periodontal pathogens in subgingival plaque: comparison of indirect immunofluorescence microscopy with bacterial culture for detection of *Actinobacillus actinomycetemcomitans*. *J Dent Res.* 1985;64:793-8.
50. Slots J, Listgarten MA. *Bacteroides gingivalis*, *Bacteroides intermedius* and *Actinobacillus actinomycetemcomitans* in human periodontal diseases. *J Clin Periodontol.* 1988;15:85-93.
51. Monteiro Mde F, Casati MZ, Taiete T, et al. Periodontal clinical and microbiological characteristics in healthy versus generalized aggressive periodontitis families. *J Clin Periodontol.* 2015;42:914-21.
52. Takeuchi Y, Umeda M, Ishizuka M, Huang Y, Ishikawa I. Prevalence of periodontopathic bacteria in aggressive periodontitis patients in a Japanese population. *J Periodontol.* 2003;74:1460-9.
53. Tomita S, Komiya-Ito A, Imamura K, et al. Prevalence of *Aggregatibacter actinomycetemcomitans*, *Porphyromonas gingivalis* and *Tannerella forsythia* in Japanese patients with generalized chronic and aggressive periodontitis. *Microb Pathog.* 2013;61-62:11-5.
54. Feng X, Zhu L, Xu L, et al. Distribution of 8 periodontal microorganisms in family members of Chinese patients with aggressive periodontitis. *Arch Oral Biol.* 2015;60:400-7.



55. Faust K, Raes J. Microbial interactions: from networks to models. *Nat Rev Microbiol.* 2012;10:538-50.
56. Faust K, Sathirapongsasuti JF, Izard J, et al. Microbial co-occurrence relationships in the human microbiome. *PLoS Comput Biol.* 2012;8:e1002606.
57. Steele JA, Countway PD, Xia L, et al. Marine bacterial, archaeal and protistan association networks reveal ecological linkages. *ISME J.* 2011;5:1414-25.
58. Chaffron S, Rehrauer H, Pernthaler J, von Mering C. A global network of coexisting microbes from environmental and whole-genome sequence data. *Genome Res.* 2010;20:947-59.
59. Barabasi AL, Albert R. Emergence of scaling in random networks. *Science.* 1999;286:509-12.

## SUPPORTING INFORMATION

Additional supporting information may be found online in the Supporting Information section.

**How to cite this article:** Liu G, Chen F, Cai Y, Chen Z, Luan Q, Yu X. Measuring the subgingival microbiota in periodontitis patients: Comparison of the surface layer and the underlying layers. *Microbiology and Immunology.* 2020;64:99-112. <https://doi.org/10.1111/1348-0421.12759>